Temperature-Dependent Anisotropy of the Penetration Depth and Coherence Length of MgB_2

J. D. Fletcher, A. Carrington, and O. J. Taylor
H. H. Wills Physics Laboratory, University of Bristol, Tyndall Avenue, BS8 1TL, United Kingdom

S. M. Kazakov and J. Karpinski
Laboratorium für Festkörperphysik, ETH Zürich, CH-8093 Zürich, Switzerland
(Received 19 January 2005; published 26 August 2005)

We report measurements of the temperature-dependent anisotropies (γ_λ and γ_ξ) of both the London penetration depth λ and the upper critical field of MgB_2. Data for $\gamma_\lambda = \lambda_c/\lambda_a$ was obtained from measurements of λ_a and λ_c on a single crystal sample using a tunnel diode oscillator technique. $\gamma_\xi = H_{c2}^{\perp c}/H_{c2}^{\parallel c}$ was deduced from field-dependent specific heat measurements on the same sample. γ_λ and γ_ξ have opposite temperature dependencies, but close to T_c tend to a common value ($\gamma_\lambda \simeq \gamma_\xi = 1.75 \pm 0.05$). These results are in good agreement with theories accounting for the two-gap nature of MgB_2.

DOI: 10.1103/PhysRevLett.95.097005 PACS numbers: 74.25.Nf, 74.70.Ad

The existence of two superconducting gaps in MgB_2 [1] leads to an unusually strong temperature dependence in the anisotropy of the upper critical field, $\gamma_\xi = H_{c2}^{\perp c}/H_{c2}^{\parallel c}$ (Refs. [2–5]). The maximum value of $\gamma_\xi \simeq 6$ is found at the lowest temperatures where it is dominated by the anisotropy in the quasi-2D σ bands. At higher temperatures, γ_ξ is substantially reduced due to the increasing contribution of the more isotropic π band [5]. The anisotropy of the penetration depth, $\gamma_\lambda = \lambda_c/\lambda_a$, is predicted to have a markedly different temperature dependence to that of H_{c2} [4,6]. At zero temperature, in the clean local limit, the anisotropy in the penetration depth is determined only by the anisotropy in the Fermi velocity v_F and not by the anisotropy in the gap [7]. Band structure calculations [8] show that the average v_F is approximately isotropic suggesting that λ is similarly isotropic at low temperature [4]. As temperature is increased it has been predicted [4,6] that γ_λ increases markedly because of the more rapid reduction of the superfluid density on the π sheets (where the gap is smaller) than on the σ sheets.

There have been several experimental measurements of the temperature dependence of γ_ξ. Although there were some disagreements in early measurements, the most recent data [2,3,9] agree well with the theoretical predictions [4,5]. Significantly less experimental data has been reported on γ_λ. Measurements of the distortion of the vortex lattice by neutron scattering [10] and scanning tunneling spectroscopy [11] suggest that at low temperature the anisotropy is small, $\gamma_\lambda = 1.2 \pm 0.1$. γ_λ has also been estimated from the anisotropy of H_{c1} ($\gamma_{H_{c1}} = H_{c1}^{\parallel c}/H_{c1}^{\perp c}$). There has been some disagreement between different studies (see Ref. [12]) but recent data [12] suggest that at low T, $\gamma_{H_{c1}} \simeq 1$ and there is an upward trend in $\gamma_{H_{c1}}$ near T_c. However, $\gamma_{H_{c1}}$ may not be simply related to γ_λ in MgB_2 because of two-gap effects. In this Letter, we present direct measurements of the temperature dependencies of λ_a and λ_c in single crystal samples of MgB_2 in the Meissner state, using a sensitive radio frequency technique. Our data show that γ_λ increases as $T \to T_c$, in agreement with theoretical predictions. Measurements of H_{c2} anisotropy in the same crystals show that the values of γ_λ and γ_ξ converge as $T \to T_c$.

Single crystals of MgB_2 were grown using a high pressure technique described elsewhere [13]. Some crystals used in this study are from the same batch as those used in de Haas–van Alphen studies [14], and are hence known to be of high quality, with mean free paths of $\ell_\pi \simeq 850$ Å, $\ell_\sigma \simeq 500$ Å. The T_c of the crystals, as determined from the midpoint of the heat capacity anomaly, was 38.3 K. Measurements of the temperature-dependent penetration depth were performed using a tunnel diode oscillator technique operating at 11.7 MHz [15]. Samples were mounted on a temperature controlled sapphire stage (base temperature 1.5 K) with the probe field aligned either into or along the boron planes.

Changes in the circuit resonant frequency ΔF are directly proportional to the change in penetration depth $\Delta\lambda$ as the sample temperature is varied. With $H \parallel c$ the shielding currents flow only in the basal plane, and hence the measured frequency shifts are directly proportional to $\Delta\lambda_a$. The constant of proportionality is determined from the geometry of the sample [16] with an accuracy of ~5–10%. For $H \perp c$ the shielding currents flow both along the c axis and in the basal plane and the measured frequency shifts contain contributions from both $\Delta\lambda_a$ and $\Delta\lambda_c$. In a rectangular sample with small to moderate demagnetizing factor [16],

$$\frac{\Delta F^{\perp c}}{\Delta F_0^{\perp c}} = \frac{\Delta\lambda_a}{t} + \frac{\Delta\lambda_c}{w}, \tag{1}$$

where $2t$ and $2w$ are the sample dimensions in the c direction and in the in-plane direction (perpendicular to the field), respectively. $\Delta F_0^{\perp c}$ is the measured frequency shift when the sample is withdrawn from the coil (note this

includes the demagnetizing factor of the sample). For this study samples with simple rectangular shapes and small aspect ratios were selected so as to maximize the c-axis contribution. The above formula neglects any contribution from the top and bottom faces of the sample. For crystals with aspect ratios equal to those reported here we expect this to be a small correction ($\lesssim 5\%$). This is supported by the fact that experimentally we find very similar values of γ_λ for samples with different aspect ratios. Most of the data presented here are for a crystal with dimensions $(0.44 \times 0.33 \times 0.15)$ mm^3 with the shortest direction being along the c axis. The accuracy of alignment with the field is estimated to be better than 5° in all cases. Corrections due to misalignment scale with $\sin^2\theta$, and are small [16]. The estimated uncertainty in the absolute values of $\Delta\lambda_a$ is 10%, and 20% for $\Delta\lambda_c$.

In Fig. 1 we show the measured temperature dependencies of both $\Delta\lambda_a$ and $\Delta\lambda_c$. In this figure we also show $\Delta\lambda_{\rm mix} = t\Delta F^{\perp c}/\Delta F_0^{\perp c}$. This quantity is directly proportional to the raw frequency shift and would equal $\Delta\lambda_a$ if the contributions from the c-axis currents were negligible. The presence of the $\Delta\lambda_c$ contributions enhances $\Delta\lambda_{\rm mix}$ with respect to $\Delta\lambda_a$. We find that the temperature dependence of $\Delta\lambda_c$ is similar to $\Delta\lambda_a$, but a factor $\sim$2 larger. This is consistent with the behavior reported previously [17], although in that study the crystals used were not of sufficiently uniform thickness to accurately determine $\Delta\lambda_c$.

The penetration depth data are more easily interpreted by calculating the normalized superfluid density $\rho = [\lambda(0)/\lambda(T)]^2$. For these calculations we take $\lambda_a(0) = \lambda_c(0) = 1000$ Å in accord with μSR and neutron studies [18–20]. We will discuss the effect of varying $\lambda_a(0)$ and $\lambda_c(0)$ later.

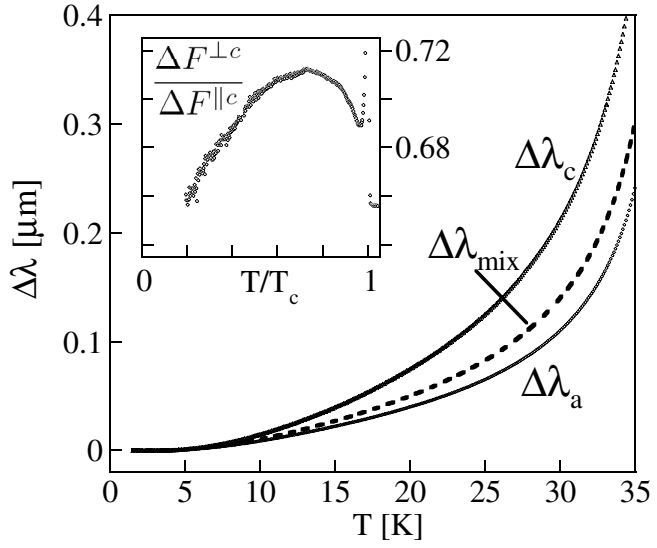

FIG. 1. Temperature dependence of $\Delta\lambda_a$, $\Delta\lambda_c$, and $\Delta\lambda_{\rm mix}$ for a single crystal of MgB_2. Inset: Ratio of the measured frequency shifts for $H \parallel c$ and $H \perp c$.

The calculated normalized superfluid densities $\rho_a(T)$ and $\rho_c(T)$ are shown in Fig. 2. $\rho_a(T)$ and $\rho_c(T)$ have quite different temperature dependencies and are both considerably different to that expected for a conventional isotropic BCS superconductor. At low temperature both superfluid densities approach unity exponentially, but at higher temperature they have a much stronger temperature dependence than that expected in the conventional case.

Previously [17], it was shown that $\rho_a(T)$ can be well described by a phenomenological two-gap model, which was first applied to MgB_2 by Bouquet *et al.* [21]. In this model, the contributions to the superfluid density from the σ and π bands (ρ_σ and ρ_π) are calculated independently using a temperature-dependent energy gap $\Delta_k(T)$ which follows the usual weak coupling BCS form but has a modified zero temperature value. These two superfluid densities are then added to give the total

$$\rho_i(T) = x_i\rho_\pi(T) + (1 - x_i)\rho_\sigma(T); \qquad (2)$$

here i refers to the crystal direction (a or c). The parameter x_i sets the relative contribution of the π band to the total normalized superfluid density. Theoretically x_i is related to band structure by [7]

$$x_i = \frac{X_i^\pi}{X_i^\sigma + X_i^\pi}, \qquad X_i^k = \int \frac{(v_i^k)^2}{v_F}\, dS_k \qquad (3)$$

where v_i^k is the i component of v_F on the sheet k ($k \in \sigma, \pi$), and the integral is over each pair of Fermi surface sheets. In MgB_2 the energy gaps are expected to deviate somewhat from the usual BCS T dependence [4,6]. A

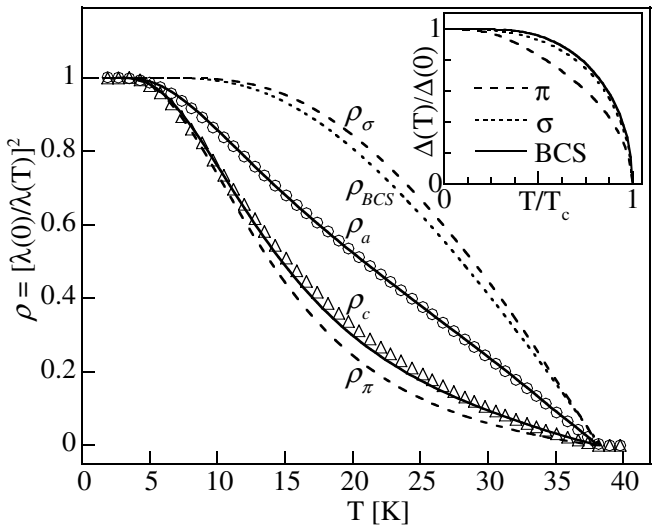

FIG. 2. In-plane and interplane normalized superfluid density, ρ_a and ρ_c calculated from $\Delta\lambda(T)$, along with fits to the two-gap model (solid lines). The behavior of ρ_σ and ρ_π deduced from the fits is also shown (dashed lines). The dotted line shows the isotropic BCS weak coupling behavior. Inset: Temperature-dependent gap functions used in the fit: (dashed and dotted lines) taken from Ref. [23]. The BCS gap function (solid line) is also shown.

simple correction [22] to the two-gap model is to use the temperature-dependent gap functions as calculated using an anisotropic strong coupling model [23] (see inset, Fig. 2).

Fits of the data to the two-gap model, calculated using $\Delta_k(T)$ from Ref. [23] are shown in Fig. 2. As discussed previously [17,22], fits to $\rho_a(T)$ give $\Delta_\pi = 29 \pm 2$ K and $\Delta_\sigma = 75 \pm 5$ K, which are in good agreement with values obtained from other measurements. The relative weight of the π band $x_a = 0.53 \pm 0.04$ is consistent with Eq. (3) using the calculated Fermi surface parameters [4].

The strong anisotropy of the σ sheets should result in the c-axis response being dominated by the more isotropic π sheets [4]. It can be seen in Fig. 2 that $\rho_c(T)$ is quite different from $\rho_a(T)$ in a manner consistent with the smaller contribution from the σ band, and appears to be mostly determined by the π band where the gap is smaller. A fit of the data to the two-gap model is shown in the figure. Here we have fixed Δ_σ and Δ_π to the values found from the fit to $\rho_a(T)$, and have set $x_c = 0.91$ as this produces the correct value for the measured anisotropy, γ_λ at T_c (see below). The fit does not change appreciably if we allow x_c to vary by $\pm$ 10%, and so is compatible with that expected from the band structure ($x_c = 0.99$) (i.e., the contribution from the σ band is not discernable).

The fit is slightly worse than for the in-plane data, and does not improve markedly if we allow the values of the adjustable parameters (x_c, Δ_σ, and Δ_π) to vary within acceptable limits. We also find that although the exact T dependence of Δ used in the model has little effect on the calculations of $\rho_a(T)$ [22]; $\rho_c(T)$ and γ_λ are somewhat more sensitive. This suggests that insufficient accuracy in the assumed form of $\Delta_\pi(T)$ is responsible for these discrepancies.

From our measurements of $\Delta\lambda_a$ and $\Delta\lambda_c$ we can calculate the anisotropy in the penetration depth as a function of temperature. This is shown in Fig. 3(a), using the same values of $\lambda_a(0)$ and $\lambda_c(0)$ as used above. Below $T \simeq 7$ K, γ_λ like $\Delta\lambda_a(T)$ and $\Delta\lambda_c(T)$ is quite temperature independent, but above this it rises monotonically reaching a value of 1.7 ± 0.3 at T_c. Changing the value of $\lambda_a(0)$ from 800 to 1200 Å or changing $\gamma_\lambda(0)$ in the range 1.0 to 1.2 does not modify the T dependence of γ_λ significantly and also has very little effect on the limiting value of γ_λ at T_c [see Fig. 3(b)]. The main uncertainty in $\gamma_\lambda(T)$ comes from the calculation of calibration factors used to extract $\Delta\lambda_a(T)$ and $\Delta\lambda_c(T)$ from the measured frequency shifts. To obtain independent estimates of the errors we have made measurements on two other crystals with different aspect ratios (w/t ranges from 8 to 2.5). These are shown in Fig. 3(c). For crystal B, γ_λ is ~10% larger at T_c but has a very similar T dependence to crystal A. Crystal C is again similar but shows more upward curvature near T_c. We note that close to T_c the results are particularly sensitive to any macroscopic inhomogeneity in the crystal (giving rise to a spread in T_c values). Data for $T/T_c > 0.95$ are particularly unreliable for this reason and are omitted from the figure.

In Fig. 3(a) we show that our data are in good agreement with the prediction of the (parameter free) strong coupling calculations of Golubov *et al.* [6] (in the clean limit). However, it should be mentioned that Ref. [6] predicts $\lambda(0)$ values which are ~2 times smaller than the experimental ones for samples of the purity we have here. We also show in this figure the calculated anisotropy of the two-gap model based on the fits to the data in Fig. 2. As mentioned above, we have adjusted x_c to give the correct value of anisotropy at T_c. As for the fits to $\rho_c(T)$, the agreement is reasonable.

For completeness we have also measured the anisotropy of H_{c2}. This was done using both torque and specific heat measurements. The heat capacity measurements were performed on the same sample (sample A) as that used for the $\lambda(T)$ measurements. For the torque measurements a different, smaller sample was used. The heat capacity c_p was

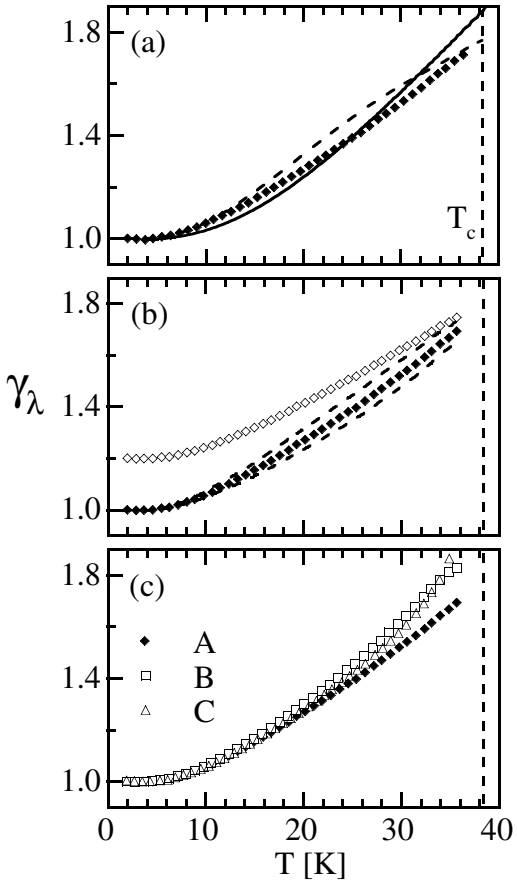

FIG. 3. (a) Penetration depth anisotropy γ_λ versus temperature for sample A (symbols). The solid/dashed lines show the behavior calculated by Golubov *et al.* [6] and the phenomenological two-gap model, respectively. (b) $\gamma_\lambda(T)$ for sample A calculated with either $\gamma_\lambda(0) = 1.0$ (solid symbols) or $\gamma_\lambda(0) = 1.2$ (open symbols). The dashed lines show the effect of changing $\lambda_a(0)$ from 1000 to 800 Å (upper curve) or 1200 Å (lower curve) [with $\gamma_\lambda(0) = 1.0$]. (c) $\gamma_\lambda(T)$ for three different samples (A,B,C).

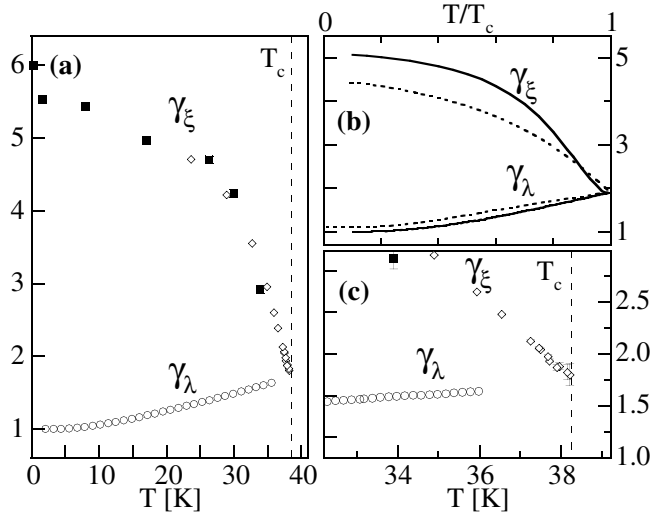

FIG. 4. (a) Temperature dependence of γ_ξ and γ_λ. For γ_ξ the open symbols are specific heat measurements and the closed symbols torque measurements. The γ_λ data are the same as in Fig. 3(a). (b) Theoretical predictions for $\gamma_\xi(T)$ and $\gamma_\lambda(T)$; solid lines: Golubov *et al.* [6] and Rydh *et al.*, dashed lines: Miranovic *et al.* [27]. (c) Detail of the experimental data in (a) close to T_c.

measured as a function of temperature by an ac technique [24] in fixed fields up to 7 T applied parallel or perpendicular to c. The jump in c_p at $T_c(H)$, was used to deduce $H_{c2}(T)$ in the two directions. In order to calculate $\gamma_\xi(T)$, we need to know H_{c2} in both field directions at a single temperature. As $H_{c2}^{\|c}$ is almost linear with T for H approximately parallel to c we interpolated this data set to give $H_{c2}^{\|c}(T)$ at the same temperature as we have data for $H \perp c$. Torque was measured as a function of H and angle at various temperatures between 0.3 and 35 K using a piezoresistive cantilever technique [25]. The angular dependence of H_{c2} was then fitted to the anisotropic Ginzburg-Landau form to give γ_ξ. Extracting H_{c2} from the torque measurements [3,14] is more difficult than for heat capacity as pinning effects, especially at low temperature, complicate the behavior close to H_{c2}. We find however, that in the region of overlap there is good agreement between the two techniques. Our results for $\gamma_\xi(T)$ shown in Fig. 4 are very similar to those reported previously [9]. In Fig. 4 we show our data for both $\gamma_\xi(T)$ and $\gamma_\lambda(T)$. Close to T_c it can be seen that both anisotropies converge to a single value. The c_p measurements are particularly well suited to determining the behavior of γ_ξ close to T_c and we find that $\gamma_\xi(T_c) = 1.75 \pm 0.05$.

In Fig. 4(b) we show two different theoretical predictions for both $\gamma_\xi(T)$ and $\gamma_\lambda(T)$. The solid lines show the results of the strong coupling calculations ($\gamma_\lambda(T)$ is as in Fig. 3 and $\gamma_\xi(T)$ is the theory of Golubov and Koshelev [26] using the fitting parameters determined by Rydh *et al.*, Ref. [9]). The dashed lines show the calculations of Miranovic, Machida, and Kogan (MMK) [27] reevaluated for a gap ratio $\Delta_\sigma/\Delta_\pi = 2.7$. Both these calculations are in good overall agreement with our data. The MMK calculation underestimates the low T value of γ_ξ because of the assumed Fermi surface shape (elliptical rather than cylindrical) but correctly predicts that $\gamma_\xi \simeq \gamma_\lambda \simeq 1.9$ at T_c. Although the calculations of Golubov *et al.* for $\gamma_\lambda(T)$ are parameter free, those for γ_ξ are not and γ_ξ and γ_λ are only equal at T_c for certain parameter values.

In conclusion, we have measured the temperature-dependent anisotropy of both the penetration depth and H_{c2} in MgB_2. As predicted by theory, they have very different temperature dependencies but tend to a common value at T_c.

We thank A. Golubov, A. Koshelev, P. Miranovic, and V. Kogan for giving us details of their calculations.

[1] See, for example, I. I. Mazin and V. P. Antropov, Physica (Amsterdam) **385C**, 49 (2003), and references therein.
[2] A. V. Sologubenko, J. Jun, S. M. Kazakov, J. Karpinski, and H. R. Ott, Phys. Rev. B **65**, 180505(R) (2002).
[3] M. Angst *et al.*, Phys. Rev. Lett. **88**, 167004 (2002).
[4] V. G. Kogan, Phys. Rev. B **66**, 020509(R) (2002).
[5] T. Dahm and N. Schopohl, Phys. Rev. Lett. **91**, 017001 (2003).
[6] A. A. Golubov, A. Brinkman, O. V. Dolgov, J. Kortus, and O. Jepsen, Phys. Rev. B **66**, 054524 (2002).
[7] B. S. Chandrasekhar and D. Einzel, Ann. Phys. (Leipzig) **2**, 535 (1993).
[8] J. Kortus, I. I. Mazin, K. D. Belashchenko, V. P. Antropov, and L. L. Boyer, Phys. Rev. Lett. **86**, 4656 (2001).
[9] A. Rydh *et al.*, Phys. Rev. B **70**, 132503 (2004).
[10] R. Cubitt *et al.*, Phys. Rev. Lett. **91**, 047002 (2003).
[11] M. R. Eskildsen *et al.*, Phys. Rev. B **68**, 100508(R) (2003).
[12] L. Lyard *et al.*, Phys. Rev. Lett. **92**, 057001 (2004).
[13] J. Karpinski *et al.*, Supercond. Sci. Technol. **16**, 221 (2003).
[14] J. D. Fletcher, A. Carrington, S. M. Kazakov, and J. Karpinski, Phys. Rev. B **70**, 144501 (2004).
[15] A. Carrington, R. W. Giannetta, J. T. Kim, and J. Giapintzakis, Phys. Rev. B **59**, R14173 (1999).
[16] R. Prozorov, R. W. Giannetta, A. Carrington, and F. M. Araujo-Moreira, Phys. Rev. B **62**, 115 (2000).
[17] F. Manzano *et al.*, Phys. Rev. Lett. **88**, 047002 (2002).
[18] C. Niedermayer, C. Bernhard, T. Holden, R. K. Kremer, and K. Ahn, Phys. Rev. B **65**, 094512 (2002).
[19] R. Cubitt, S. Levett, S. L. Bud'ko, N. E. Anderson, and P. C. Canfield, Phys. Rev. Lett. **90**, 157002 (2003).
[20] K. Ohishi *et al.*, J. Phys. Soc. Jpn. **72**, 29 (2003).
[21] F. Bouquet *et al.*, Europhys. Lett. **56**, 856 (2001).
[22] A. Carrington and F. Manzano, Physica (Amsterdam) **385C**, 205 (2003).
[23] A. Brinkman *et al.*, Phys. Rev. B **65**, 180517(R) (2002).
[24] A. Carrington *et al.*, Phys. Rev. B **55**, R8674 (1997).
[25] C. Rossel *et al.*, J. Appl. Phys. **79**, 8166 (1996).
[26] A. A. Golubov and A. E. Koshelev, Phys. Rev. B **68**, 104503 (2003).
[27] P. Miranovic, K. Machida, and V. G. Kogan, J. Phys. Soc. Jpn. **72**, 221 (2003); P. Miranovic (Private communication).